

Supplementary Information for

Iron oxidation dynamics vs. temperature of synthetic potassic-ferro-richterite: a XANES investigation

G. Della Ventura,^{a,b} F. Galdenzi,^a G. Cibin,^c R. Oberti^d, Wei Xu^{e,f}, S. Macis^{b,g} and A. Marcelli^{b,f}

^a Department Sciences, University of Roma Tre, Rome, Italy

^b INFN-LNF, P.O.Box 13, 00044 Frascati (Rome), Italy

^c CNR-Istituto di Geoscienze e Georisorse, Pavia, Italy

^d Diamond Light Source, Harwell Science and Innovation Campus, Didcot, UK

^e BSRF, Institute of High Energy Physics, Beijing, 100049, P.R. China

^f RICMASS, Rome International Center for Materials Science Superstripes, Rome, Italy

^g Università di Tor Vergata, Via della Ricerca Scientifica 1, 00133 Roma, Italy

Comparison of the M(1), M(2) and M(3) octahedral sites geometries vs. temperature

In the following Table we list the changes in the individual M-O lengths of the three independent M(1-3) octahedra, measured before the annealing experiment and after the annealing. Data are from Oberti *et al.* [1], and point out how all changes in the average distances are well within 5% but for the contraction of the M(1)-O3 distance that is ~8%. This strong contraction is mainly due to the shortening of the M(1)-O(3) bond required to maintain local electroneutrality at O(3) oxygen after the loss of the proton.

Table S1 – Variation of the individual and averaged bond distances (Å) and of the bond angular variance (OAV, ° [2]) for the M sites due to thermal expansion and to the deprotonation process. * = corrected for riding motion.

Bond distance (Å)	RT before annealing	523 K	Δ%	RT after annealing	Δ%
M(1) - O(1) x2	2,118	2,116*	-0,09	2,056	-2,93
M(1) - O(2) x2	2,098	2,102*	0,19	2,109	0,48
M(1) - O(3) x2	2,134	2,148*	0,66	1,955	-8,39
<M(1)-O>	2,116	2,122*	0,28	2,040	-3,59
OAV M(1)	38,66	33,46	-13,45	38,90	0,62
M(2) - O(1) x2	2,188	2,200*	0,55	2,177	-0,50
M(2) - O(2) x2	2,131	2,141*	0,50	2,138	0,28
M(2) - O(4) x2	1,992	1,998*	0,30	1,981	-0,55
<M(2)-O>	2,104	2,113*	0,43	2,098	-0,29
OAV M(2)	42,56	44,48	4,51	55,19	29,68
M(3) - O(1) x4	2,124	2,131*	0,33	2,170	2,17
M(3) - O(3) x2	2,091	2,098*	0,33	2,028	-3,01
<M(3)-O>	2,113	2,120*	0,33	2,123	0,47
OAV M(3)	55,70	51,10	-8,26	60,89	9,32

XAS - pre-edge analysis

At the Fe K-edge, the pre-edge feature arises from the transition from the 1s to the 4p-3d hybridized orbitals that are highly sensitive to the coordination and to the electronic state of the photo-absorbing atom. To isolate and analyse the pre-edge features, we first subtracted an appropriate baseline to the spectrum. To fit the baseline at the pre-edge, different approaches have been considered in the literature such as: two Gaussians [3,4], a pseudo-Voigt with a 50:50 Gaussian-

Lorentzian contribution [5] and an arctangent [6]. The latter, although difficult to apply when two electronic configurations occur, is certainly the best choice to subtract the main edge absorption jump [7]. Before the baseline subtraction with an arctangent function all absorption spectra were normalized to the atomic absorption edge. To this purpose, we used the Demeter package for XAS data analysis [8]. Each spectrum from RT temperature up to HT, i.e., in the range $176 < T < 523$ °C, was normalized to 0 before the absorption edge and to 1 above the edge at ~ 7250 eV using Athena.

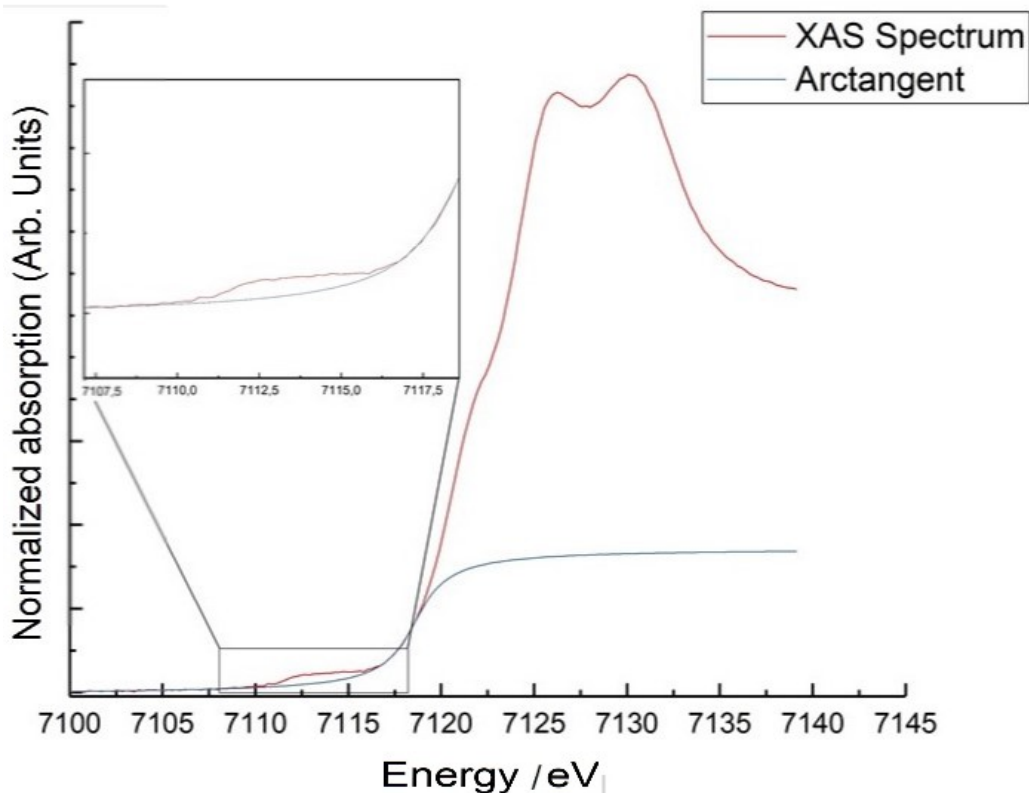


Figure S1- Example of the procedure used for the background subtraction at the pre-edge, after the normalization of the absorption spectrum (this spectrum refers to 176 °C). The inset shows a zoom of the pre edge region.

We extracted the pre-edge features from each spectrum using the arctangent function in the energy region 7100-7120 eV. A selected example is given in Figure S1. In each spectrum the arctangent function was shifted to follow the shift of the Fe K-edge vs. temperature.

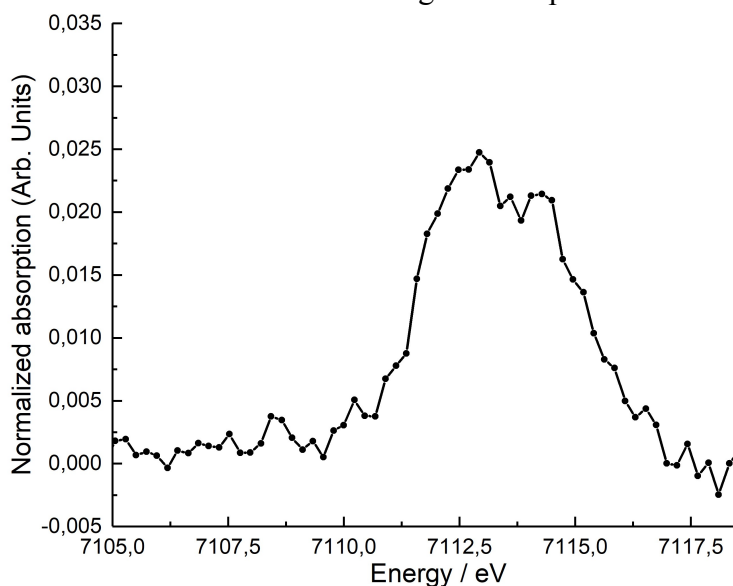


Figure S2 – A magnified figure of the pre-edge feature of the spectrum showed in Figure S1 after the background subtraction.

A representative example of the result obtained after the background subtraction (spectrum collected at $T = 174$ °C) is given in Figure S2. To reduce the S/N ratio, three consecutive spectra,

e.g., 167, 176 and 185 °C were summed. After the background subtraction, all spectra in the pre-edge region were decomposed using 4 contributions. Also for the pre-edge fit different functions have been proposed such as Gaussian [6] and pseudo Voigt [1,5,10] with a variable Gaussian/Lorentzian ratio based on the energy resolution available. The choice is based on the consideration that at the K-edge two electronic transitions are expected, from 1s to 3d-4p hybridized orbitals, for a Fe atom in an octahedral coordination [3]. In our system we have at least four components, i.e., two for Fe^{2+} and two for Fe^{3+} electronic configurations.

Table S1 – Initial values of the fit of the pre-edge, the mean energy position of each component considering all fitted spectra and the related standard deviations. G stands for Gaussian, PV for pseudo-Voigt.

	Initial Energy (eV)	Mean Energy position (eV)	σ (eV)
1 st component G	7112,2	7112,09	0,19
2 nd component G	7113,4	7113,32	0,24
3 rd component G	7114,3	7114,52	0,12
4 th component G	7115,0	7115,37	0,19
1 st component PV	7112,2	7112,36	0,09
2 nd component PV	7113,4	7113,35	0,15
3 rd component PV	7114,3	7114,29	0,12
4 th component PV	7115,0	7115,10	0,19

In order to choose the best function to use to fit our data (i.e., Gaussian vs. pseudo-Voigt) we considered the edge shift at the intensity of 0.6 and 0.8. The results are plotted in Figure 4 in the manuscript. Data vs. temperature have been fitted with a Boltzmann sigmoid to evaluate the temperature of the oxidation process.

We have also calculated the Fe^{3+}/Fe_{tot} fitting the pre-edge with 4 Gaussians and with 4 pseudo-Voigt with a 80:20 Gaussian/Lorentzian ratio trying to account for the detector resolution, which in our case does not allow to separate the two electronic configurations. In our fit, the width of each component was constrained to be constant (1.4 eV) [1]. The energy position of each component was left free to vary in a range of ± 0.4 eV from the initial value shown in table S1. To set the initial values for the fit we considered the centroid energy range of the Fe^{2+} and Fe^{3+} pre-edge configurations according to a previous study performed on different iron bearing minerals [1]. Table 1 gives the mean energy position of each component for all temperatures for both cases. Two representative examples of the fit of the pre-edge with 4 Gaussians and with 4 pseudo-Voigt with a 80:20 Gaussian/Lorentzian ratio are showed in Figure S3.

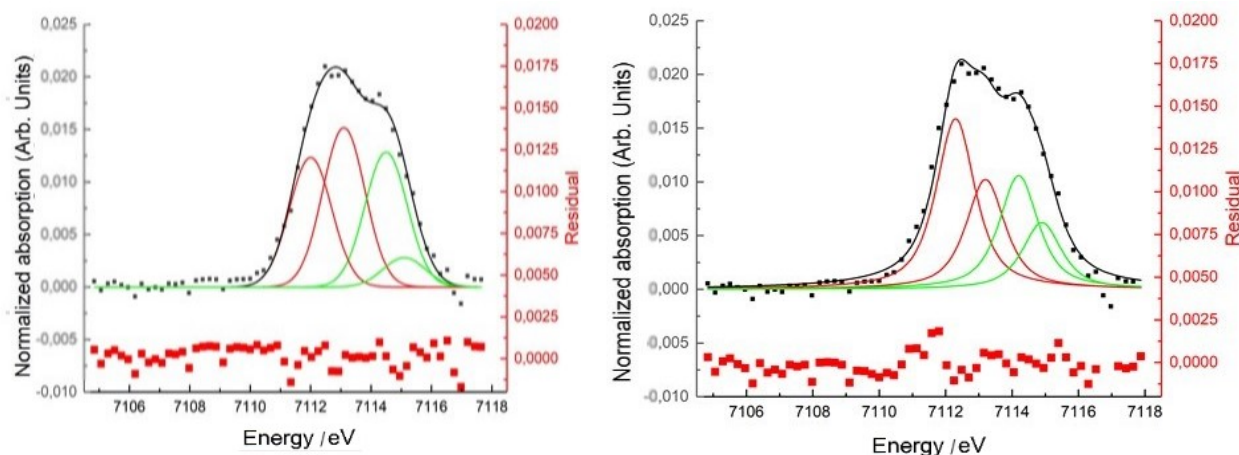


Figure S3 - Example of the fits of the pre-edge feature (spectrum at 176 °C). The red and the green components are associated to the Fe^{2+} and to the Fe^{3+} , respectively. The red dots in the bottom show the residual, i.e., the difference between experimental data (black squares) and fit (black line). The left panel show the Gaussian fit while the right panel shows the pseudo-Voigt fit.

The resulting intensities (area) of the four components, A_1 and A_2 for Fe^{2+} , A_3 and A_4 for Fe^{3+} have been used to calculate the Fe^{3+}/Fe_{tot} ratio for each temperature using the formula:

$$R = \frac{A_3 + A_4}{A_1 + A_2 + A_3 + A_4} = \frac{Fe^{3+}}{Fe_{tot}}$$

The residual, i.e., the difference between the calculated vs. experimental points (Figure S5) has been used to evaluate the validity of this approach. We evaluated the areas of residual by integrating the modulus of the difference between the pre-edge experimental values and the fit for each temperature. In Figure S4 we compare the behaviour of the residuals for both Gaussian vs. pseudo-Voigt fits. The residuals are clearly lower (~ 2.5) for the first case over all the temperature range supporting this method for the fit of spectra collected with this experimental resolution.

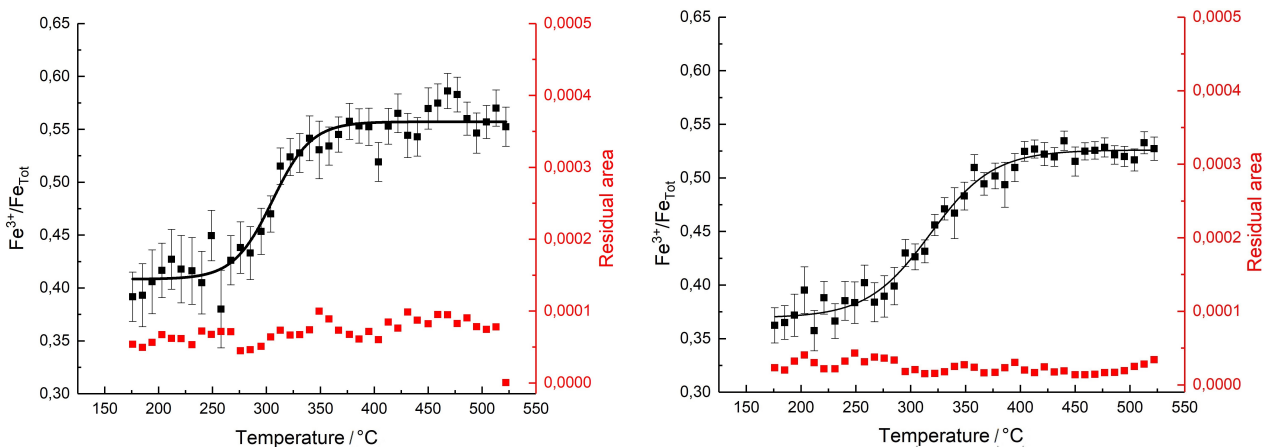


Figure S4 – The behaviour of the Fe^{3+}/Fe_{tot} ratio (black) vs. temperature and the corresponding residual area (red) obtained from the pre-edge fitting procedures. On the left is represented the ratio obtained from the pseudo-Voigt fit while on the right the same ratio obtained with the fit with four Gaussian functions.

We also compared the results of the Fe^{3+}/Fe_{tot} of these two fit with the values obtained considering the energy shift behaviour probed at 0.6 and 0.8. All values obtained are showed in Figure S5.

The temperature calculated by Gaussian contributions is higher than that calculated using pseudo-Voigts, and fall between those obtained by the energy shift methods within the error bars. Taking into account also the experimental resolution, the result supports our choice to prefer the Gaussian functions to fit the pre-edge features.

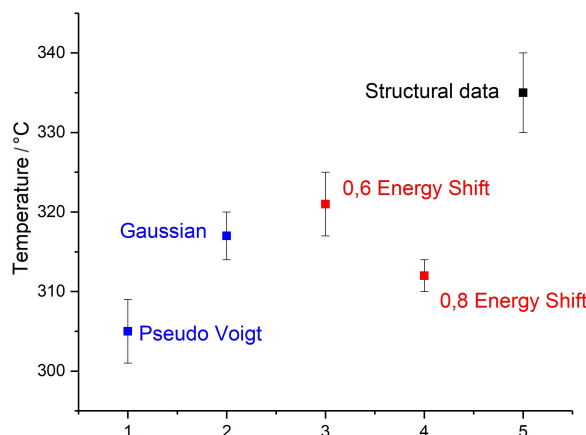


Figure S5 – The oxidation temperatures calculated by the energy shift method (red) and the pseudo-Voigt and the Gaussian fits (blue). The temperature calculated by XRD structural analysis from [7] is also plotted (black).

Density Functional Theory (DFT) calculations

The band structure and density of states have been calculated starting from the in situ XRD data of Oberti et al. [1] and using the density functional theory based on the generalized gradient approximation (GGA) of Perdew-Burke-Ernzerhof (PBE) as implemented in the Vienna *Ab-initio* Simulation Package (VASP) [10].

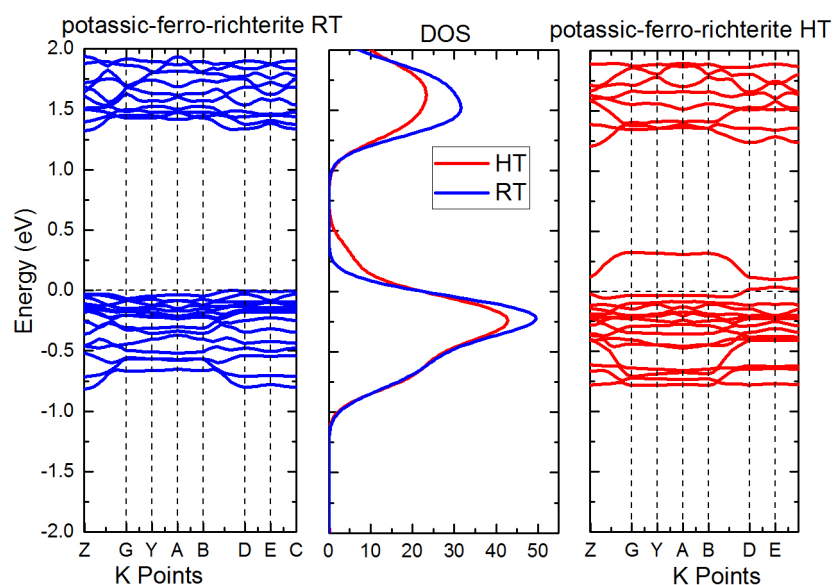


Figure S6 Band structure and density of states for potassic-ferro-richterite at RT (left) and at HT (right).

The electron and core interactions are included using the frozen-core projector augmented wave (PAW) method, with the plane-wave cutoff energy fixed at 400 eV for all the phases refined from XRD data. The lattice constants and the atom coordinates were optimized until the force on each atom converged to less than 10 meV/Å. The Monkhorst–Pack scheme is used to sample the Brillouin zone. The structures were fully relaxed with a mesh of $2 \times 1 \times 4$, and the mesh of k space was increased to $5 \times 3 \times 9$ and $9 \times 5 \times 11$ in the static and density of state (DOS) calculations, respectively. The number of bands per k point was set to 10 during the electronic band structure calculations. The band structure and the density of states obtained are compared in Figure S6.

References

- [1] R. Oberti, M. Boiocchi, M. Zema, G. Della Ventura, Synthetic potassic-ferro-richterite: *I. Composition, crystal-structure and HT behaviour by in operando single-crystal X-ray diffraction*. *Can. Mineral.*, 2016, 54, 353-369.
- [2] K. Robinson, G.V. Gibbs, P.H. Ribbe, *Quadratic elongation: a quantitative measure of distortion in coordination polyhedra*. *Science* **172**, 567–570 (1971).
- [3] L. Galois, G. Calas, M.A. Arrio, *High-resolution XANES Spectra of Iron in Minerals and Glasses: Structural Information from the Pre-edge Region* *Chemical Geology* 174, 307-319 (2001)
- [4] M. Wilke, G.M. Partzsch, R. Bernhardt, D. Lattard, *Determination of the iron oxidation state in basaltic glasses using XANES at the K-edge*, *Chemical Geology* 213, 71-87 (2004)
- [5] N. Bolfan-Casanova, M. Muñoz, C. McCammon, E. Deloué, A. Fêrot, S. Demouchy, L. France, D. Andrault, S. Pascarelli, *Ferric iron and water incorporation in wadsleyite under hydrous and oxidizing conditions: A XANES, Mössbauer, and SIMS study*, *American Mineralogist* 97, 1483-1493 (2012)

- [6] M.S. Platunov, N.V. Kazak, Yu.V. Knyazev, L.N. Bezmaternykh, E.M. Moshkina, A.L. Trigub, A.A. Veligzhanin, Y.V. Zubavichus, L.A. Solovyov, D.A. Velikanov, S.G. Ovchinnikov, *Effect of Fe-substitution on the structure and magnetism of single crystals $Mn_{2-x}Fe_xBO_4$* . *J. Cryst. Growth* 475, 239-246 (2017)
- [7] A. Mottana, X-ray absorption spectroscopy in mineralogy: *Theory and experiment in the XANES region*, *EMU Notes in Mineralogy* 6, chapt. 12, 465-552 (2004)
- [8] B. Ravel and M. Newville, *ATHENA, ARTEMIS, HEPHAESTUS: data analysis for X-ray absorption spectroscopy using IFEFFIT*, *J. Synchr. Rad.* 12, 537–541 (2005)
- [9] G. Kresse, J. Furthmüller, *Efficiency of ab-initio total energy calculations for metals and semiconductors using a plane-wave basis set*, *Comput. Mat. Sci.* 12, 15-50 (1996)
- [10] P.E. Petit, F. Farges, M. Wilke, V.A. Solé, *Determination of the iron oxidation state in Earth materials using XANES pre-edge information*. *J. Synchrotron Rad.*, **8**, 952-954 (2001).